

# A Design of Hand Rehabilitation Exoskeleton Mechanism Adapted to Different Finger Lengths

Chao Qin, Peng Li, Xiaojun Yang, Bing Li

Harbin Institute of Technology (Shenzhen)

Shenzhen, 518055, China

Email: yangxiaojun@hit.edu.cn

**Abstract:** Stroke can cause the neurological function of the brain hemisphere or brain stem to be blocked, which in turn causes partial loss of function of the hands and feet. This paper presents a hand rehabilitation exoskeleton mechanism with an adjusted locking device to adapt to different finger lengths. The biological characteristics of the finger are analyzed to obtain the motion parameters of the finger. The presented mechanism is optimized for its rod length by the fgoalattain function optimization method. This is done for the exoskeleton mechanism could drive the finger to reach the ideal bending angle. A proof-of-concept plastic prototype was fabricated, and the experimental results demonstrates the potential of this mechanism.

**Keywords:** Hand rehabilitation; Exoskeleton mechanism; Rod length optimization; Rehabilitation experiment

## I. INTRODUCTION

China's aging population is showing an increasing trend every year, and the number of people affected is increasing year by year. The impact of stroke on life is huge. In the early stage of stroke, if the patient is given early rehabilitation training, this can enhance the patient's self-care ability, and can greatly reduce the chance of disability [1]. Through the training of the hand rehabilitation institution, not only can the treatment intensity be guaranteed, but also the economic burden can be reduced. There are two main trends in the field of rehabilitation therapy. One is the constraint-induced motion therapy proposed by Professor Edward Taub [2], and the other is the continuous passive activity theory CPM [3]. It can be learned from domestic and foreign literatures that CPM theory is applied more widely.

At present, in the field of hand rehabilitation robots, many aspects of robotic arm rehabilitation therapy [4]–[6], including clinical tests [7]–[9], have been reported. representative research results include the hand function rehabilitation robot HX[10] developed by the University of Pisa, Italy. The robot uses a back structure, and the fingertip joint of the exoskeleton of the mechanism is concentric with the human hand joint. The patient has a better recovery experience. Harvard University has developed a rehabilitation glove [11][12] that combines software technology with an exoskeleton robot. The robotic glove uses a soft actuator, which is composed of an elastomeric cavity and a fiber reinforcement. In the case of fluid pressurization, the fiber reinforcement can cause specific bending, stretching, and twisting. However, this design requires further robustness and actuator fatigue life testing, and requires individual customization for different finger lengths of the patient, which results in an expensive

price. Nowadays, domestic achievements in the field of hand rehabilitation robots have also achieved certain results. Huazhong University of Science and Technology has developed a hand-functioning rehabilitation robot [13] using artificial muscle as a driving device, which makes the mechanism more comfortable and safe. This mechanism overcomes the shortcomings of traditional artificial muscle single movement. A hand-functioning rehabilitation robot developed by Beijing University of Aeronautics and Astronautics [14][15], which is driven by a rope. The drive motor is separated from the finger exoskeleton so that the robot is not limited by the placement space. In summary, the existing hand rehabilitation exoskeleton structure is complex, and needs to be customized according to the user's finger parameters, which is not only poorly adaptable, but also expensive.

In this article we have designed an exoskeleton structure that can accommodate different finger lengths based on a simple four-bar mechanism. As shown in Fig. 1, the structure is driven by the twisted rope to avoid the safety problem of excessive rigidity caused by the direct drive of the motor, and the feedback mechanism is established by using the Hall angle sensor and the film pressure sensor. This structure is simple and easy to implement customization requirements. The Section 2 of this paper provides a succinct analysis of the biological characteristics of the finger. In Section 3 of this paper, the structural parameters of the exoskeleton mechanism for hand function rehabilitation were designed and the rod length was optimized. Finally, a new exoskeleton driving method based on twisted rope was proposed. In Section 4 of this paper, the adaptability of the hand function rehabilitation exoskeleton to different finger lengths and the range of joint motion were verified by experiment.

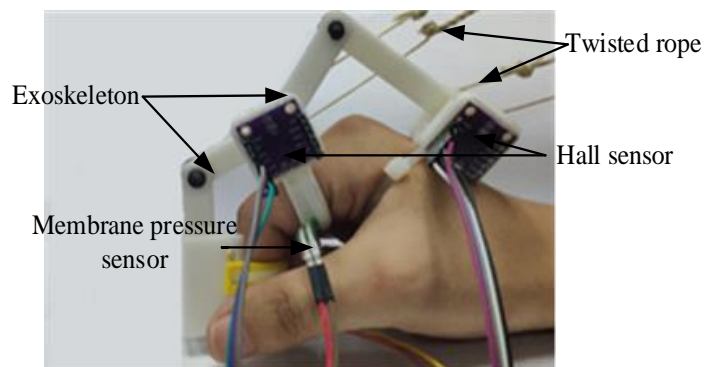


Fig.1 The design of the hand function rehabilitation exoskeleton

## II. BIOLOGICAL CHARACTERISTICS OF THE FINGER

In general, each joint of a finger can only perform one or two movements. As shown in Fig. 2, the hand bone is composed of the finger bone and the metacarpal bone. Normal people remove the thumb and the remaining four fingers have the same structure. Including metacarpophalangeal (MCP), proximal interphalangeal (PIP), and distal interphalangeal (DIP) [16], MCP joints can perform vertical palm bending/stretching and parallel The two degrees of freedom of the palm's abduction/adduction movement constitute such a form of exercise. PIP and DIP joints only have one degree of freedom, so they can only be bent/stretched.

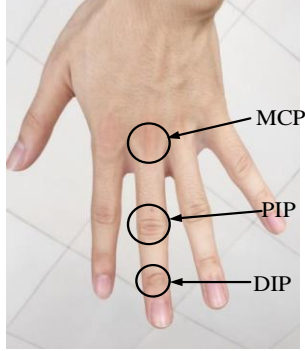


Fig. 2 Human hand joint structure model

## III. THE DESIGN OF HAND FUNCTION REHABILITATION EXOSKELETON SYSTEM

### A. Structural Plan of Hand Rehabilitation Exoskeleton Mechanism

Fig. 3 is a schematic diagram of the single-finger rehabilitation exoskeleton mechanism of the hand. C is the finger MCP joint, and F is the PIP joint, which can be equivalently regarded as the rotation pair. The whole body can be regarded as a planar 4R mechanism, which is composed of OABC rotating pairs. The OABC rotating pairs is formed in series with a planar RRRP mechanism composed of BEGF motion pairs, where B is a composite hinge. In the mechanism, the rotating pairs O and B are the main driving pairs, and the mechanism is a 2 DOF mechanism. The planar 4R mechanism produces two component forces at the point of B, one being the force in the direction of the vertical finger and the other being the traction in the direction of the finger. Increasing the transmission angle reduces the traction along the direction

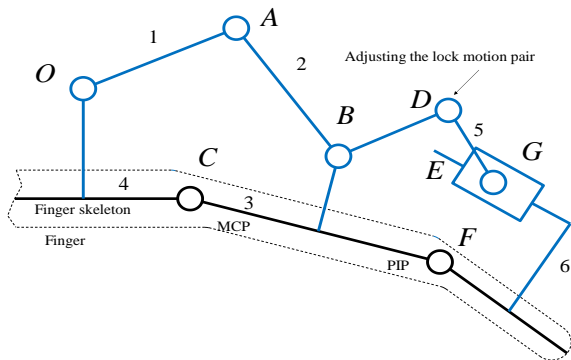


Fig. 3 Schematic diagram of hand rehabilitation exoskeleton structure

of the finger. Therefore, increasing the transmission angle is one of the main criterion for the design of the mechanism. The rotating pair F is the PIP joint of the finger, and the mechanism designs the E portion as the moving pair, so that the traction force along the finger direction becomes the moving driving force of the slider, which can cause no damage to the human finger. The BD rod and the DE rod of the structure can be adjusted at the point of D, and are locked after adjustment. The purpose of this design is to adjust the angle between the two rods according to the difference of the human finger, and has good adaptability to fingers of different sizes.

### B. Parameter Design and Optimization of Rod Length

According to the length of the normal adult finger structure obtained by consulting the relevant literature and the diameter parameters of each knuckle joint [17], the rod length of the design mechanism is required. In order to ensure the transmission performance of the structure and the rationality of the structural design, the parameters of the functional rehabilitation exoskeleton structure should be designed and optimized. The optimization of the rod length is optimized by using the nonlinear programming solution function fgoalattain in the Matlab optimization toolbox. Fig. 4 shows the movement of the MCP articulated rod OA to the limit position, where  $c$  is the height of the pedestal and is constant  $\gamma_{\min}$  is the minimum value of the transmission angle and  $\varphi_{\max}$  is the maximum value of bending angle. At this time, the transmission angle moves to the minimum value, as in (1), at which time the bending angle of the proximal phalanx reaches the maximum value, with (2):  $l_1, l_2, l_4, l_{31}$  represent the length of the sports pairs and  $l_{OC}, l_{AC}, l_{BC}$  represent the distance from each rotating pair of the mechanism to the MCP joint.

$$\begin{aligned} l_{OC} &= \sqrt{c^2 + l_4^2} \\ l_{AC} &= \sqrt{c^2 + (l_1 - l_4)^2} \\ l_{BC} &= \sqrt{c^2 + l_{31}^2} \\ \gamma_{\min} &= \cos^{-1} \left( \frac{l_2^2 + l_{BC}^2 - l_{AC}^2}{2l_2l_{BC}} \right) \end{aligned} \quad (1)$$

$$\varphi_{\max} = \cos^{-1} \left( \frac{l_{AC}^2 + l_{BC}^2 - l_2^2}{2l_{AC}l_{BC}} \right) - \sin^{-1} \frac{c}{a} + \tan^{-1} \frac{c}{l_{31}} \quad (2)$$

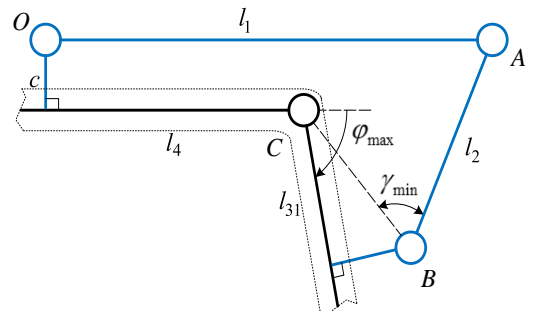


Fig. 4 Drive component OA rod movement to the extreme position map

The target solved in the solution process is not unique, because the mathematical model is built according to the above analysis, and the model with multiple objective functions is solved. Through the analysis of the limit position of the mechanism, the following two goals are achieved during the whole movement: (1) To make the MCP joint movement limit at around  $80^\circ$ ; (2) When the whole mechanism is in transmission, the minimum value of the transmission angle should be made to obtain better transmission performance.

To simplify the calculation, the parameters are dimensionless. we let  $l_{31}/l_{31}=1$ ,  $l_1/l_{31}=x(1)$ ,  $l_2/l_{31}=x(2)$ ,  $l_4/l_{31}=x(3)$ ,  $c/l_{31}=y(1)$ , then the design variables can be obtained:  $X=[x(1) \ x(2) \ x(3)]$ .

The angle of rotation of the finger and the minimum transmission angle are determined by the length of the rod in the four-bar mechanism. For these two design elements, the designed objective function can be obtained:

$$f_1(x)=|\varphi-\frac{4}{9}\pi| \quad (3)$$

$$f_2(x)=|\frac{\pi}{2}-\gamma| \quad (4)$$

In the optimization, according to the parameters required by the transmission, the range of the target function is determined in detail:

1) The movement of the finger should be as close as possible to  $80^\circ$  and  $1^\circ$  up and down:

$$-0.01745 \leq f_1(x) \leq 0.01745$$

2) Available from the minimum transmission angle conditions of the design:

$$0 \leq f_2(x) \leq 0.6981$$

In order to guarantee the optimization results, you need to constrain the known conditions, you need to meet the following constraints:

$$g_1(x)=1-x(1) \leq 0$$

$$g_2(x)=1-x(2) \leq 0$$

$$g_3(x)=1-x(3) \leq 0$$

$$g_3(x)=1-x(3) \leq 0$$

$$g_4(x)=-1+x(1)-x(2)-x(3) \leq 0$$

$$g_5(x)=-1-x(1)+x(2)-x(3) \leq 0$$

$$g_6(x)=1+x(3)-x(1)-x(2) \leq 0$$

So we get the MCP limit position structure parameters of TABLE I.

TABLE I  
MCP JOINT LIMIT POSITION STRUCTURE PARAMETERS

$l_{31}/\text{mm}$	$l_1/\text{mm}$	$l_2/\text{mm}$	$l_3/\text{mm}$	$\varphi_{\max}/^\circ$	$\gamma_{\min}/^\circ$
20	44.96	32.36	23.03	80.17	53.33

For the PIP joint of the human finger, the PIP joint

range of the normal person is larger, and the limit position reaches  $110^\circ$ , as shown in Fig. 5, the BD rod moves to the extreme position. For the patient, the joint bending angle of  $90^\circ$  fully meets the exercise requirements.  $d_6$  is the distance between the sliding pair and the PIP joint and  $\varphi_{\max}$  is the maximum bending angle of the PIP joint. Set the value of the joint bending angle to move around  $90^\circ$ . When the finger moves to the limit, make sure that the slider is more than 10 mm away from the PIP joint. Only in this way can the normal bending motion of the PIP joint be satisfied. According to these two goals, two objective functions (5), (6) are established:

$$d_6=\sqrt{(l_{52}\sin\frac{4}{9}\pi-c)^2-(l_{51}-l_{52}\cos\frac{4}{9}\pi-l_{32})^2-c^2} \quad (5)$$

$$\varphi_{\max}=\tan^{-1}\left(\frac{c}{d_6}\right)+\tan^{-1}\left(\frac{l_{52}\sin\frac{4}{9}\pi-c}{l_{51}-l_{52}\cos\frac{4}{9}\pi-l_{32}}\right) \quad (6)$$

To simplify the calculation, let  $l_{32}/l_{32}=1$ ,  $l_{51}/l_{32}=z(1)$ ,

$l_{52}/l_{32}=z(2)$ , and then get the variable:  $Z=[z(1) \ z(2)]$ .

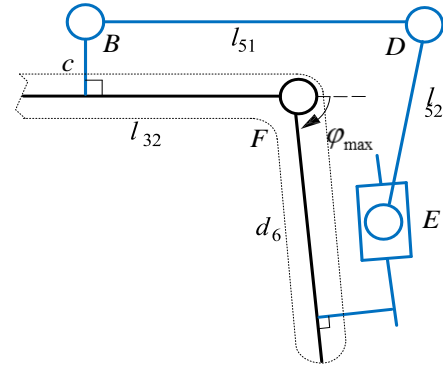


Fig. 5 Drive component BD rod movement to the extreme position map

The objective function designed by this:

$$h_1(x)=|12.5-d_6| \quad (7)$$

$$h_2(x)=|\varphi-\frac{\pi}{2}| \quad (8)$$

1) The sliding sub-limit position value  $d_6$  varies by about 1 mm:

$$-1 \leq h_1(x) \leq 1$$

2) The target value of  $\varphi$  is about  $90^\circ$ , which is allowed to float up and down by  $1^\circ$  during design:

$$-0.01745 \leq h_2(x) \leq 0.01745$$

In order to guarantee the optimization results, we need to constrain the known conditions, we need to meet the following constraints:

$$g_1(x)=1-z(1) \leq 0$$

$$g_2(x)=1-z(2) \leq 0$$

So we get the PIP limit position structure parameters of TABLE II.

TABLE II  
PIP JOINT LIMIT POSITION STRUCTURE PARAMETERS

$l_{32}/\text{mm}$	$l_{51}/\text{mm}$	$l_{52}/\text{mm}$	$\varphi_{\max}/^{\circ}$	$d_6/\text{mm}$
20	40.6	28.8	90.75	12.78

### C. The Driven Method

As a relatively new driving method, twisted rope has not been widely used in the field of rehabilitation robots. Driven by a twisted rope, not only can the quality of the mechanism be reduced, the rigidity of the mechanism can be reduced, and safer human-computer interaction can be realized. The vibration problem caused by direct driving of the motor can be avoided. In addition, the twisted rope drive is cheaper and more suitable for promotion. The principle of the driving method is shown in Fig. 6. One end of a plurality of cables of the same material is fixed on the rotating shaft of the motor, and the other end of the rope is fixed on the load. Fig7. shows the twisted-line drive design of the hand-function rehabilitation mechanism. When the motor rotates, the cables will be twisted and twisted together. The length of the cable is twisted together due to mutual twisting, so that the cable is generally shortened, providing a certain pulling force to the load, and pulling the load to move axially along the direction of the motor. Since the size of the hand is limited, if the rod is selected to be driven, the motor needs to be fixed on the arm, which will directly affect the comfort of the stroke patient and also affect the recovery time of the patient. Due to its unique advantages, the twisted rope method has a high reduction ratio and light weight. Therefore, in practical applications, this paper can adjust the length of the twisted rope within a certain range, and can

adjust the position of the motor according to the change of the environment. Therefore, in the selection of the motor, the motor with small size and light weight can be applied to complete the driving of the hand function rehabilitation robot.

According to the above analysis, the mechanism model of the hand function rehabilitation exoskeleton of Fig. 8 is designed. Fig. 8 a) is a three-dimensional structure diagram of a single finger, and Fig. 8 b) is a three-dimensional structure diagram of the entire finger.

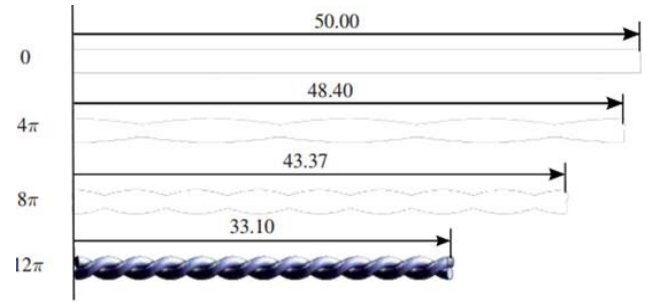


Fig.6 The schematic of the twisted rope driven

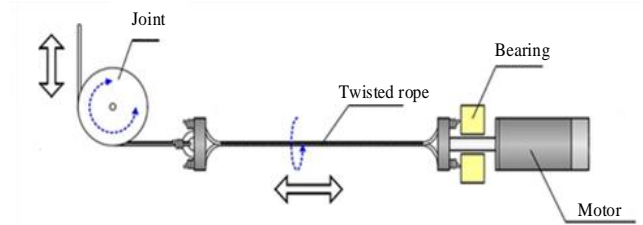
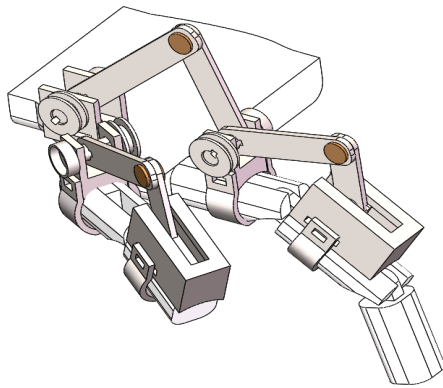
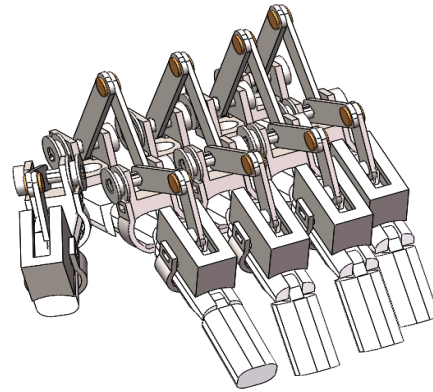


Fig.7 The structure of the twisted rope driven

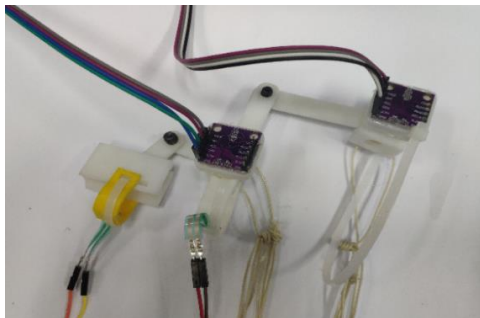


a) 3D figure of single finger

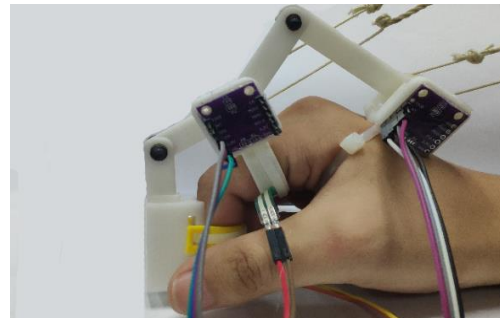


b) Three-dimensional drawing of five fingers

Fig.8 Hand function rehabilitation exoskeleton mechanism model



a) Finger exoskeleton structure



b) Schematic diagram of wearing exoskeleton

Fig. 9 The platform of the finger exoskeleton experiment



#### IV. HAND FUNCTION REHABILITATION EXOSKELETON MECHANISM PERFORMANCE VERIFICATION

##### A. Construction of The Experimental Platform

Fig. 9 shows the construction of the test bench. The experimental platform of the hand function rehabilitation robot mainly includes: DC power supply, exoskeleton structure, drive motor, hardware software and the like. Use the cable tie to secure the exoskeleton to your finger. The Arduino drives the motor and uses a twisted rope for power transmission. During the rehabilitation process, it is necessary to know the range of motion that the patient's fingers can accept. Using the active motion rehabilitation method, the Hall sensor is used to collect the angular range of the actual movement of the finger, and the motor feedback is controlled by the signal fed back by the lamination sensor. During the active motion, the pressure value of the laminating sensor can be detected to determine the degree of participation in the active motion. Fig.10 shows the pressure felt by the laminating sensor. Fig.11 shows the angle at which the actual transformed joint can be bent, which shows that the structure can achieve active finger rehabilitation.

##### B. Human Hand Adaptive Performance Verification

For different patients, the length of the fingers is different. One criterion for measuring the structure of the hand function is whether it is suitable for different patients. The fixed distance on the proximal finger joint is fixed. The distal locking joint uses the adjusted locking device to adapt the hand function rehabilitation robot to fingers of different lengths, and adjusts the two by adjusting the self-locking

bolt between the two rods. As shown in Fig.12, the angle between the members to accommodate fingers of different lengths.

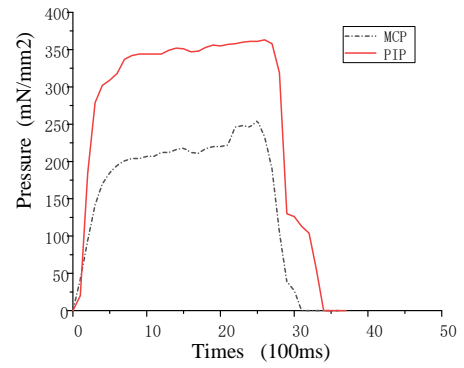


Fig.10 Pressure at the MCP and PIP joints

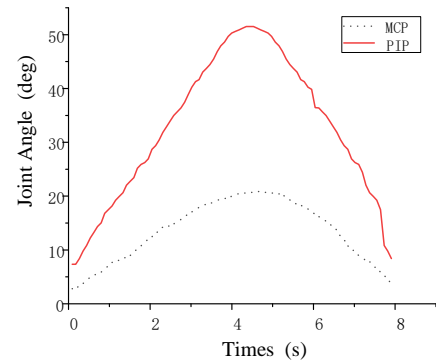


Fig.11 The bending angle of MCP and PIP joint

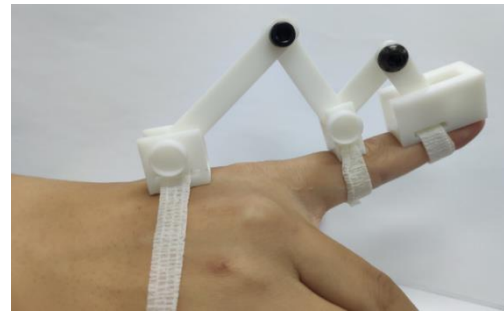
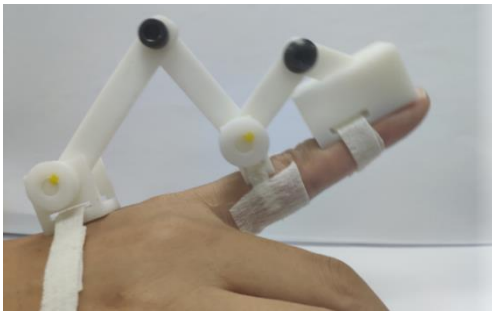
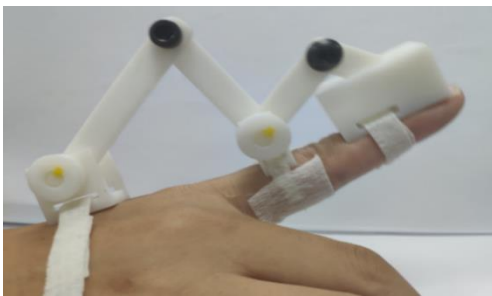
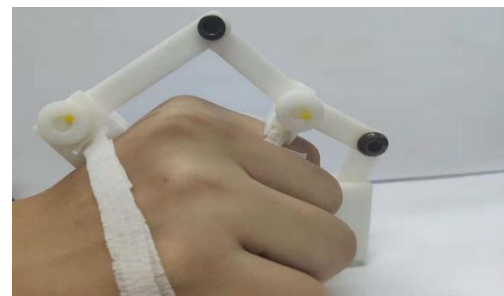


Fig. 12 Finger adaptive experiment



a) Joint starting position



b) Joint limit position

Fig.13 Experimental verification of joint motion range

TABLE III  
FINGER WEAR / REMOVE ROBOT JOINT ACTIVITY ANGLE

joint	Mode of motion	Free finger movement	Wear exoskeleton sports
MCP joint	Bend/stretch	75	68
PIP joint	Bend/stretch	92	85

### C. Joint Motion Range Performance Verification

In order to achieve the desired healing effect of the patient, it is necessary to know how much the range of motion of the finger joint can be reached after wearing the finger exoskeleton. As described above, in the experiment, six groups of normal persons were measured to wear the exoskeleton and unloaded. The maximum bending angle of the finger's MCP and PIP fingers in the exoskeleton, Fig.13 is one set of experimental procedures, and TABLE III. is the average of the results of the finger angle bending experiment.

As can be seen from the results in the table, the angle of movement after wearing the exoskeleton device is smaller than the angle of free movement of the finger, mainly because the exoskeleton of the wearer limits the movement of a part of the finger. For normal people, the number of the movement of the finger bends to the limit is very small, so the range of motion reached by the fingers after wearing the exoskeleton is appropriate for the patient.

### V.CONCLUSION

The planar 4R and RRPR exoskeleton structures are designed for the MCP joint and the PIP joint of the finger respectively. The exoskeleton structure is simple and easy to implement. For different patient's finger lengths, the mobile sub-adjustment locking device is designed. It is verified by experiments that the exoskeleton structure has excellent adaptability to different finger lengths.

By analyzing the biological characteristics of the finger, the motion parameters of the finger are obtained, and the scale optimization function of the exoskeleton mechanism is established as the design target. The optimal rod length is obtained by the fgoalattain function optimization method, and the exoskeleton that the mechanism drives the finger to the desired bending angle is verified by experiments.

### REFERENCE

- [1] Tao Quan, "Hand injury rehabilitation," 2006:18-36.
- [2] Miltner WH, Bauder H, Sommer M, Dettmers C, Taub E, "Effects of Constraint-Induced Movement Therapy on Patients with Chronic Motor Deficits after Stroke : a Replication," 1999,30(3) :586-92.
- [3] R.B.Salter,P.Field."The Effects of Continuous Compression on Living Articular Cartilage,"The Journal of Bone and Joint Surgery. 1960,42(1) :31~32.
- [4] C. Carignan and M. Liszka, "Design of an arm exoskeleton with scapula motion for shoulder rehabilitation," in Proc. IEEE Int. Conf. Robotics Automation (ICRA), 2005, pp. 524-531.
- [5] A. Gupta and M. K. O'Malley, "Design of a haptic arm exoskeleton for training and rehabilitation," IEEE/ASME Trans. Mechatronics, vol. 11, no. 3, pp. 280-289, Jun. 2006.
- [6] D. J. Reinkensmeyer, C. T. Pang, J. A. Nessler, and C. C. Painter, "Webbased telerehabilitation for the upper extremity after stroke," IEEE Trans. Neural Syst. Rehabil. Eng., vol. 10, no. 2, pp. 102-108, Jun. 2002.
- [7] L. E. Kahn, M. L. Zygmans, W. Z. Rymer, and D. J. Reinkensmeyer, "Effect of robot-assisted and unassisted exercise on functional reaching in chronic hemiparesis," in Proc. 23rd IEEE Eng. Med. Biol. Conf., 2001, pp. 1344-1347.
- [8] R. M. Mahoney, H. F. Machiel Van der Loos, P. S. Lum, and C. Bugar, "Robotic stroke therapy assistant," Robotica, vol. 21, pp. 33-44, 2003.
- [9] P. R. Culmer, A. E. Jackson, S. Makower, R. Richardson, J. A. Cozens, M. C. Levesley, and B. B. Bhakta, "A control strategy for upper limb robotic rehabilitation with a dual robot system," IEEE/ASME Trans. Mechatronics, vol. 15, no. 4, pp. 575-585, Aug. 2010.
- [10] Cempini M, Cortese M, Vitiello N, "A Powered Finger-Thumb Wearable Hand Exoskeleton with Self-Aligning Joint Axes," IEEE/ASME Transactions on Mechatronics, 2015, 20(2) :705-716.
- [11] Polygerinos P, Wang Z, Galloway K C, et al, "Soft robotic glove for combined assistance and at-home rehabilitation," 2015, 73: 135- 143.
- [12] Wang Z, Polygerinos P, Overvelde J T B, et al, "Interaction Forces of Soft Fiber Reinforced Bending Actuators," IEEE/ASME Transactions on Mechatronics, 2017, 22(2): 717-727.
- [13] Wu J, Huang J, Wang Y, et al, "A Wearable Rehabilitation Robotic Hand Driven by PM-TS Actuators[J]. Intelligent Robotics and Applications," 2010 : 440-450.
- [14] Wang J, Li J, Zhang Y, et al, "Design of an Exoskeleton for Index Finger Rehabilitation," Engineering in Medicine and Biology Society, 2009. EMBC 2009. Annual International Conference of the IEEE. IEEE, 2009:5957-5960.
- [15] Wang S, Li J, Zhang Y, et al, "Active and Passive Control of An Exoskeleton with Cable Transmission for Hand Rehabilitation," Biomedical Engineering and Informatics, 2009. BMEI'09. 2nd International Conference on. IEEE, 2009:1-5.
- [16] Hasegawa Y, Tokita J, Kamibayashi K, et al, "Evaluation of Fingertip Force Accuracy in Different Support Conditions of Exoskeleton," Robotics and Automation (ICRA), 2011 IEEE International Conference on. IEEE, 2011:680-685.
- [17] J. W. Lee, K. Rim, "Maximum Finger Force Prediction Using a Planar Simulation of the Middle Finger. Proceedings of Instrumentation Mechanical Engineering," 1990, 204:160-178.